A Phase Field Crystal Approach for Particles in a Flowing Solvent

Simon Praetorius,* Axel Voigt*

A number of dynamic density functional theories (dDFTs) have been developed to describe the dynamics of the one-particle density of atomic fluids. We review an approach that accounts for particle advection by a flowing solvent, and make further approximations using a locally advected phase-field-crystal model which in turn is coupled with a Navier–Stokes equation. In particular we apply the approach to Brownian particles (e.g., coarse grained polymer coils) in a solvent flowing around various obstacles (e.g., colloidal particles). We compare the bow wave in the density distribution of particles in front of the obstacles as well as the wake behind it. The results qualitatively agree with full dDFT results and simulations based on the underlying Brownian dynamics. The much lower computational cost of the phase field crystal approach provides an efficient way to couple fluid flow around macroscopic fixed or moving particle with interactions of particles in the solvent.

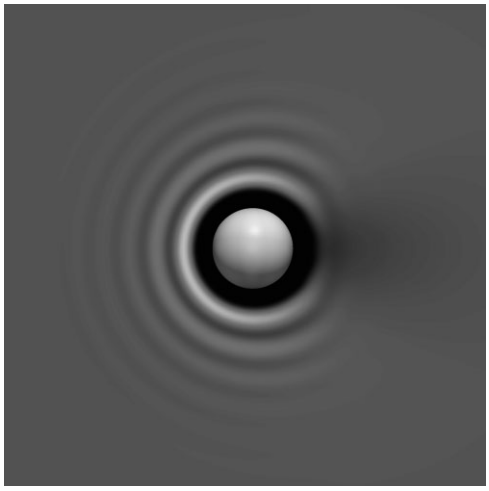

Introduction

Binary mixtures of colloids and non-adsorbing polymer coils are ideal model systems for the study of phase behavior and equilibrium as well as non-equilibrium physics of multicomponent systems.

The generalization of classical density functional theory (DFT) to the case of non-equilibrium situation, known as dynamic density functional theory (dDFT), was first introduced by Marconi and Tarazona,[1] and was recently extended to driven systems[2] in the advected dynamic density functional theory (adDFT). The authors used this method to model colloidal particles moving through a polymer solution, or conversely, the flow of polymer particles around a fixed macroscopic particle. The colloid deforms the flow field, as it has radius of hydrodynamic interaction with the solvent greater than 0.

Earlier studies of a similar system with conventional DFT[3] neglected this deformation and are therefore only valid for small obstacles of radius $R \ll d$, where d represents the size of the polymer particles. A full dDFT model including the advection of the solvent particles was analyzed by ref.[2]

Simple flow fields around a colloidal particle with radius R at low Reynolds number are given by the solution of the Stokes equation around a spherical obstacle at the origin:

$$\mathbf{u}(\mathbf{r}) = \mathbf{c} - \frac{3R}{4\|\mathbf{r}\|}\left(1 + \frac{R^2}{3\|\mathbf{r}\|^2}\right)\mathbf{c} + \frac{3R}{4\|\mathbf{r}\|^3}\mathbf{r}(\mathbf{r}\cdot\mathbf{c})\left(\frac{R^2}{\|\mathbf{r}\|^2} - 1\right), \quad (1)$$

with $\mathbf{c} = c^{\infty}\,\mathbf{e}_x$ the velocity at infinity distance from the obstacle. For $R = 0$ this reduces to the uniform flow $\mathbf{u}(\mathbf{r}) = \mathbf{c}$.

S. Praetorius
Institut für Wissenschaftliches Rechnen, Technische Universität Dresden, 01062 Dresden, Germany
E-mail: simon.praetorius@tu-dresden.de
A. Voigt
Institut für Wissenschaftliches Rechnen and Center for Advanced Modeling and Simulation, Technische Universität Dresden, 01062 Dresden, Germany
E-mail: axel.voigt@tu-dresden.de

DOI: 10.1002/mats.201100004

More complex situations with more colloidal particles that are not fixed but can move independently, are difficult or impossible to calculate analytically. Numerical solutions of the Stokes equation have to be used. For non-stationary flow fields a direct coupling of the equations of fluid dynamics to the equations of the simulation of interacting polymer particles in the solvent would be necessary. Such coupling is crucial for the inclusion of the hydrodynamic forces between polymer coils exerted on the solvent.

In this paper we present an approximation of the dDFT using a phase field crystal (PFC) model, and motivated by refs.[2,3] extend it by a transport term to approximate the generalized adDFT. In contrast to dDFT equations the PFC model is given by a differential equation and can easily be coupled to other equations like the aforementioned Navier–Stokes equations of fluid dynamics.

The paper is organized as follows: in the next section the model is derived starting from the Langevin equation of motion for an ensemble of advected interacting Brownian particles. Using various approximations we have obtained an advected PFC-model, which is coupled to a Navier–Stokes equation. In Computational Results Section simulation results for the polymer density around a colloidal particle were shown. We have considered the bow wave in the density distribution of particles in front of the obstacles as well as the wake behind it and have compared the results with full dDFT results and simulations based on the underlying Brownian dynamics. The density profile is analyzed in terms of different velocities and different radii of the obstacle. In Conclusion Section we have drawn conclusions.

Model Derivation

A continuum model considering the particle density in a flowing solvent is derived starting from an atomistic theory as motived by ref.[1]

Fokker–Planck Equation

We consider the Langevin equation of motion for an ensemble of N advected interacting Brownian particles with position coordinates $\vec{\mathbf{r}} = \{\mathbf{r}_1, \mathbf{r}_2, \dots, \mathbf{r}_N\}$, and mass m, immersed in an incompressible fluid.

$$\begin{aligned}\partial_t \mathbf{r}_i &= \mathbf{u}(\mathbf{r}_i,t) + \frac{1}{\gamma}\left(F_i(\vec{\mathbf{r}},t) + \eta_i(t)\right)\\ &= \mathbf{u}(\mathbf{r}_i,t) - \frac{1}{\gamma}\left(\nabla_{\mathbf{r}_i}\left[\sum_i V_1(\mathbf{r}_i,t) + \sum_{i<j} V_2(\|\mathbf{r}_i - \mathbf{r}_j\|)\right]\right) + \overline{\eta}_i(t)\end{aligned} \tag{2}$$

with the external potential $V_1(\mathbf{r}_i, t)$, the pair interaction potential $V_2(\|\mathbf{r}_i - \mathbf{r}_j\|)$, flow field $\mathbf{u}(\mathbf{r}_i, t)$ and a noise term $\overline{\eta}_i(t)$. The potential terms sum up to the deterministic force F_i acting on the ith particle. Equation (2) is a stochastic differential equation for each particle in the system.

The corresponding Fokker–Planck equation for a probability density, $W(\vec{\mathbf{r}}, t)$, which determines the probability of finding the set of N particles around the positions $\mathbf{r}_1, \dots, \mathbf{r}_N$ reads:

$$\begin{aligned}&\partial_t W(\vec{\mathbf{r}},t) = \mathcal{L}_S W(\vec{\mathbf{r}},t) \quad \text{with}\\ &\mathcal{L}_S(\cdot) = \sum_i \nabla_{\mathbf{r}_i} \cdot \left[\left(-\mathbf{u}(\mathbf{r}_i,t) - \frac{1}{\gamma}F_i(\vec{\mathbf{r}},t) + k_B T \nabla_{\mathbf{r}_i}\right)(\cdot)\right]\end{aligned} \tag{3}$$

with initial conditions $W(\vec{\mathbf{r}}, t_0) = \delta(\vec{\mathbf{r}} - \vec{\mathbf{r}}_0)$ and appropriate boundary conditions.

Because we are not interested in the individual position of all particles, but rather the probability of finding any particle at a given position, we can integrate Equation (3) over $N-1$ of the N variables to obtain a one-particle density distribution. We introduce the n-particle density $\rho^{(n)}$ by integrating the probability density $(N-n)$-times:

$$\rho^{(n)}(\mathbf{r}_1, \dots, \mathbf{r}_n, t) = \frac{N!}{(N-n)!}\int \cdots \int W(\vec{\mathbf{r}},t)\, \mathrm{d}\mathbf{r}_{n+1} \dots \mathrm{d}\mathbf{r}_N.$$

Dropping the superscript for the one-particles density $\rho^{(1)} =: \rho$ and the subscript in the positions one obtains the continuity equation:

$$\partial_t \rho(\mathbf{r},t) + \nabla \cdot (\rho(\mathbf{r},t)\,\mathbf{u}(\mathbf{r},t)) = -\nabla \cdot \mathbf{j}(\mathbf{r},t) \tag{4}$$

with

$$\begin{aligned}\gamma \mathbf{j}(\mathbf{r},t) &= -\rho(\mathbf{r},t)\nabla V_1(\mathbf{r},t) - k_B T \nabla \rho(\mathbf{r},t)\\ &\quad - \int \rho^{(2)}(\mathbf{r},\mathbf{r}',t)\nabla V_2(\|\mathbf{r}-\mathbf{r}'\|)\,\mathrm{d}\mathbf{r}'.\end{aligned} \tag{5}$$

If we neglect the pair-interaction term containing the two-particle density $\rho^{(2)}$, Equation (4 and 5) reduce to Fick's diffusion equation in a flowing heat bath:

$$\begin{aligned}&\partial_t \rho(\mathbf{r},t) + \nabla \cdot (\rho(\mathbf{r},t)\,\mathbf{u}(\mathbf{r},t)) = -\nabla \cdot \mathbf{j}(\mathbf{r},t)\\ &\Gamma^{-1}\mathbf{j}(\mathbf{r},t) = -\rho(\mathbf{r},t)\nabla U_1(\mathbf{r},t) - \nabla \rho(\mathbf{r},t)\end{aligned} \tag{6}$$

with an external potential $U_1 := (k_B\, T)^{-1} V_1$ and diffusion coefficient $\Gamma := k_B\, T \gamma^{-1}$. This equation models the flow of non-interacting particles.

Dynamic Density Functional Theory

In classical dDFT the flux $\mathbf{j}$ is related to the gradient of the variational derivative of an energy functional $\mathcal{F}[\rho(\mathbf{r})] := \mathcal{F}_{\mathrm{id}}[\rho(\mathbf{r})] + \mathcal{F}_{\mathrm{ext}}[\rho(\mathbf{r})] + \mathcal{F}_{\mathrm{ex}}[\rho(\mathbf{r})]$. The functional

consists of an ideal solution part $\mathcal{F}_{id}[\rho(\mathbf{r})] = \int k_B T\rho(\mathbf{r})(\ln(\rho(\mathbf{r})\Lambda^d)-1)\,d\mathbf{r}$, where Λ is the thermal wavelength, a description for an external potential $\mathcal{F}_{ext}[\rho(\mathbf{r})] = \int \rho(\mathbf{r},t)V_1(\mathbf{r},t)\,d\mathbf{r}$, and the excess free energy for particle interactions $\mathcal{F}_{ex}[\rho(\mathbf{r})]$, that is unknown for general systems. The authors of ref.[2] used this relation for the adDFT to obtain the evolution equation,

$$\partial_t\rho(\mathbf{r},t) + \nabla\cdot(\rho(\mathbf{r},t)\mathbf{u}(\mathbf{r})) = \nabla\cdot\left(\gamma^{-1}\rho(\mathbf{r},t)\nabla\frac{\delta\mathcal{F}[\rho(\mathbf{r},t)]}{\delta\rho(\mathbf{r},t)}\right). \tag{7}$$

Equation (7) still contains the unknown free energy part $\mathcal{F}_{ex}$ and further approximations are necessary. One approach to obtain $\mathcal{F}_{ex}$ is the mean-field approximation for very soft interactions $\mathcal{F}_{ex}[\rho] \approx (1/2)\iint \rho(\mathbf{r})\rho(\mathbf{r}')\nabla V_2(\|\mathbf{r}-\mathbf{r}'\|)\,d\mathbf{r}\,d\mathbf{r}'$.

In ref.[2] this approach is used to obtain a dDFT for particles in a flowing solvent. Even if the approach is only valid for potential flows, in ref.,[3] situations are described where it gives good approximations in cases without detailed balance. This is confirmed in ref.[2] by considering Stokes flows.

We will follow this route and further approximate Equation (7). To derive more efficient models which allow us to simulate more complex problems we consider a different way to approximate $\mathcal{F}_{ex}$. Known approximations for hard and soft particles include those based on the Rosenfeld fundamental measure theory, weighted density approximation,[4] and the Ramakrishnan–Yussouff (RY) approximation.[5] In this work we use the RY approximation.

Phase-Field-Crystal Model

Consider the relative density deviation from a constant reference liquid density: $\delta\rho(\mathbf{r}) := \rho(\mathbf{r})-\rho_L$. The excess free part of the energy can be approximated in the RY-approximation by expansion around the liquid density ρ_L up to second order, in the sense of generalized gradient expansions:

$$\begin{aligned}
&\mathcal{F}_{ex}[\rho(\mathbf{r})]-\mathcal{F}_{ex}[\rho_L] =: \Delta\mathcal{F}_{ex}[\rho(\mathbf{r})]\\
&\approx \int \delta\rho(\mathbf{r})\frac{\delta\mathcal{F}_{ex}[\rho_L]}{\delta\rho(\mathbf{r})}\,d\mathbf{r} + \frac{1}{2}\iint \delta\rho(\mathbf{r})\delta\rho(\mathbf{r}')\frac{\delta^2(\mathcal{F}_{ex}[\rho_L])}{\delta\rho(\mathbf{r})\delta\rho(\mathbf{r}')}\,d\mathbf{r}\,d\mathbf{r}'\\
&= -k_BT\int\delta\rho(\mathbf{r})c^{(1)}(\mathbf{r},\rho_L)\,d\mathbf{r} - \frac{k_BT}{2}\iint\delta\rho(\mathbf{r})c^{(2)}(\mathbf{r},\mathbf{r}',\rho_L)\delta\rho(\mathbf{r}')\,d\mathbf{r}\,d\mathbf{r}'
\end{aligned}$$

with the direct correlation functions, given by $c^{(1)}(\mathbf{r},\rho) = (-1/k_BT)(\delta\mathcal{F}_{ex}[\rho]/\delta\rho)$ and $c^{(2)}(\mathbf{r}_1,\mathbf{r}_2,\rho) = (\delta c^{(1)}(\mathbf{r}_1,\rho)/\delta\rho(\mathbf{r}_2)) = (-1/k_BT)(\delta^2(\mathcal{F}_{ex}[\rho])/\delta\rho(\mathbf{r}_1)\delta\rho(\mathbf{r}_2))$. In the liquid reference fluid another form of $c^{(1)}$ can be found: $c^{(1)}(\mathbf{r},\rho_L) = \ln(\rho_L\Lambda^d)-(\mu_L/k_BT)$ with μ_L the constant chemical potential of the reference liquid.

The ideal gas part $\mathcal{F}_{id}$ of the energy can be rewritten as:

$$\begin{aligned}
&\mathcal{F}_{id}[\rho(\mathbf{r})]-\mathcal{F}_{id}[\rho_L] =: \Delta\mathcal{F}_{id}[\rho(\mathbf{r})]\\
&= k_BT\int\delta\rho(\ln(\rho_L\Lambda^d)-1) + \rho(\mathbf{r})\ln\left(\frac{\rho(\mathbf{r})}{\rho_L}\right)d\mathbf{r}.
\end{aligned}$$

Combining both, ideal gas and excess free part of the energy (relative to the reference liquid state), results in:

$$\begin{aligned}
\Delta\mathcal{F}_{id}[\rho(\mathbf{r})] + \Delta\mathcal{F}_{ex}[\rho(\mathbf{r})] = k_BT\int &\underbrace{\delta\rho(\mathbf{r})\left(\frac{\mu_L}{k_BT}-1\right)}_{f_1(\rho(\mathbf{r}))}\\
&+ \underbrace{\rho(\mathbf{r})\ln\left(\frac{\rho(\mathbf{r})}{\rho_L}\right)}_{f_2(\rho(\mathbf{r}))} - \underbrace{\frac{1}{2}\int\delta\rho(\mathbf{r})\bar{c}^{(2)}(\mathbf{r},\mathbf{r}',\rho_L)\delta\rho(\mathbf{r}')\,d\mathbf{r}'}_{f_3(\rho(\mathbf{r}))}d\mathbf{r}.
\end{aligned}$$

Because V_2 depends on the distance $\|\mathbf{r}-\mathbf{r}'\|$ only, this property is assumed to be true also for the direct pair correlation function, especially in the liquid phase, so $c^{(2)}(\mathbf{r},\mathbf{r}',\rho_L) =: \bar{c}^{(2)}(\|\mathbf{r}-\mathbf{r}'\|)$ and the rotational symmetry of $\bar{c}^{(2)}$ follows immediately.

Now consider the Fourier transformed correlation function by rewriting $f_3(\rho)$ as convolution $f_3(\rho(\mathbf{r})) = (1/2)\delta\rho(\mathbf{r})[\bar{c}^{(2)} * \delta\rho](\mathbf{r})$. The correlation-function is rotationally symmetric. This leads to a simplification of the Fourier-transform of $\bar{c}^{(2)}$ to:

$$\Im[\bar{c}^{(2)}] =: \hat{c}(\mathbf{k}) = \int_{\mathbb{R}^d}\bar{c}^{(2)}(\|\mathbf{r}\|)\cos(\mathbf{k}\cdot\mathbf{r})\,d\mathbf{r}.$$

Expanding $\hat{c}$ around $\mathbf{k}_0 = 0$[6] leads to:

$$\hat{c}(\mathbf{k}) = \hat{C}_0 + \mathbf{k}^2\hat{C}_2 + \mathbf{k}^4\hat{C}_4 + \ldots$$

with $\mathbf{k}^m := \sum_i k_i^m$. The coefficients with odd derivatives vanish, due to the choice of the expansion point. We can now write the Fourier transform of f_3 as:

$$\begin{aligned}
\Im[f_3(\rho)](\mathbf{k}) &= \frac{1}{2\cdot(2\pi)^d}[\hat{\delta}\rho * (\hat{c}\cdot\hat{\delta}\rho)](\mathbf{k})\\
&= \frac{1}{2\cdot(2\pi)^d}[\hat{\delta}\rho * ((\hat{C}_0 + \hat{C}_2(\cdot)^2 + \hat{C}_4(\cdot)^4 + \ldots)\cdot\hat{\delta}\rho)](\mathbf{k}) =: \hat{f}_3(\rho).
\end{aligned}$$

The inverse Fourier transform leads to the real space approximation, by truncating the expansion at fourth order:

$$\Im^{-1}\left[\hat{f}_3(\rho)\right](\mathbf{r}) \approx \frac{1}{2}\delta\rho(\mathbf{r})(\hat{C}_0 - \hat{C}_2\Delta(\cdot) + \hat{C}_4\Delta^2(\cdot))\delta\rho(\mathbf{r}).$$

To relate the parameters $\hat{C}_i$ to those of other models which assume constant mobility in Equation (7) on the right-hand side (e.g., the PFC2-model[7]), the ideal solution term in the energy is expanded around the mean density $\bar{\rho}$. We introduce a new variable $\phi(\mathbf{r},t) := (\rho(\mathbf{r},t)-\bar{\rho})/\bar{\rho} = (\delta\rho(\mathbf{r},t)-\bar{\rho})/\bar{\rho} + \rho_L/\bar{\rho}$, the dimensionless *density modulation*, and truncate the expansions at fourth order. For ϕ the property $\int\phi(\mathbf{r},t)\,d\mathbf{r} = 0$ holds. The expansions of $f_i(\rho)$ in terms of ϕ, neglecting all linear terms

because they vanish on differentiation, yield:

$$\begin{aligned}
&\frac{1}{\overline{\rho}}(f_1(\rho(\mathbf{r}))-f_1(\overline{\rho})) = \phi(\mathbf{r},t)\left(\frac{\mu_L}{k_BT}-1\right) = (\text{linear term})\\
&\frac{1}{\overline{\rho}}(f_2(\rho(\mathbf{r}))-f_2(\overline{\rho})) \approx \frac{1}{2}\phi(\mathbf{r},t)^2-\frac{1}{6}\phi(\mathbf{r},t)^3\\
&+\frac{1}{12}\phi(\mathbf{r},t)^4 + (\text{linear terms})\\
&\frac{1}{\overline{\rho}}(f_3(\rho(\mathbf{r}))-f_3(\overline{\rho})) \approx \frac{\overline{\rho}}{2}\phi(\mathbf{r},t)(\hat{C}_0-\hat{C}_2\Delta+\hat{C}_4\Delta^2)\phi(\mathbf{r},t)\\
&+(\text{linear terms}).
\end{aligned}$$

The third term in the energy, $\Delta\mathcal{F}_{ext}[\rho] = \int \delta\rho V_1 =: \int f_4(\rho)$, containing the external potentials, can also be expressed in terms of ϕ as $(1/\overline{\rho})(f_4(\rho(\mathbf{r}))-f_4(\overline{\rho})) = \phi(\mathbf{r},t)V_1(\mathbf{r},t)$. Finally we can define the total free energy relative to the mean density by summation of the energy parts: $(1/\overline{\rho})(\Delta\mathcal{F}[\rho(\mathbf{r},t)]-\Delta\mathcal{F}[\overline{\rho}]) = (1/\overline{\rho})(\mathcal{F}[\rho(\mathbf{r},t)]-\mathcal{F}[\overline{\rho}]) \approx \mathcal{F}_1[\phi(\mathbf{r},t)]$ with:

$$\begin{aligned}
\frac{\mathcal{F}_1[\phi(\mathbf{r},t)]}{k_BT} :=& \int \frac{1}{2}\phi(\mathbf{r},t)^2-\frac{1}{6}\phi(\mathbf{r},t)^3+\frac{1}{12}\phi(\mathbf{r},t)^4\,\mathrm{d}\mathbf{r}\\
&-\int \frac{\overline{\rho}}{2}\phi(\mathbf{r},t)(\hat{C}_0-\hat{C}_2\Delta+\hat{C}_4\Delta^2)\phi(\mathbf{r},t)\,\mathrm{d}\mathbf{r}\\
&+\int \frac{1}{k_BT}M(\phi(\mathbf{r},t))V_1(\mathbf{r},t)\,\mathrm{d}\mathbf{r}
\end{aligned} \tag{8}$$

where $M(\phi) := \rho = (\phi+1)\overline{\rho}$, and the notation $\mathcal{F}_1$ comes from the original name *PFC1-model* in ref.[7] Now the evolution equation with respect to $\phi(\mathbf{r},t)$ can be written as:

$$\begin{aligned}
&\partial_t\phi(\mathbf{r},t)+\nabla\cdot(\phi(\mathbf{r},t)\mathbf{u}(\mathbf{r})) = \nabla\cdot\left\{\gamma^{-1}M(\phi)\nabla\frac{\delta\mathcal{F}_1[\phi(\mathbf{r},t)]}{\delta\phi(\mathbf{r},t)}\right\}\\
&= k_BT\nabla\cdot\left\{\gamma^{-1}M(\phi)\nabla(\phi(\mathbf{r},t)-\frac{1}{2}\phi(\mathbf{r},t)^2+\frac{1}{3}\phi(\mathbf{r},t)^3\right.\\
&\left.+(k_BT)^{-1}M'(\phi)V_1(\mathbf{r},t)-\overline{\rho}(\hat{C}_0-\hat{C}_2\Delta\phi(\mathbf{r},t)+\hat{C}_4\Delta^2\phi(\mathbf{r},t)))\right\}
\end{aligned} \tag{9}$$

This evolution equation is an approximation of the dynamic density functional evolution Equation (7) obtained by expansion of the correlation function. It is related to the classical PFC equation, extended by an advection term and non-constant mobility, and was first derived by Elder and Grant.[8]

To obtain this standard form we introduce a new variable $\varrho := (1-2\phi)\overline{\varrho}$ and perform a re-parametrization to new parameters r and $\overline{\varrho}$. The number of parameters is reduced by setting the lattice constant to 1, i.e., to fix the ratio $2|\hat{C}_4| : \hat{C}_2 \stackrel{!}{=} 1$. Stability considerations give the sign of the last parameter, i.e., $\mathrm{sign}(\hat{C}_4) = -1$. This leads to the parameter relations:

$$\hat{C}_0 := \hat{C}_2\left(\frac{9}{2}-\frac{1}{2}(1+r)\right), \quad \hat{C}_2 := \frac{1}{6\overline{\rho}\overline{\varrho}^2}, \quad \hat{C}_4 := -\frac{1}{2}\hat{C}_2$$

Inserting this into the energy (8) and neglecting linear and constant terms we arrive at the proposed standard formulation that is the base for our simulations:

$$\begin{aligned}
\frac{\mathcal{F}_1[\varrho(\mathbf{r},t)]}{k_BT} = C\int &\frac{1}{2}\varrho(\mathbf{r},t)(r+(1+\Delta)^2)\varrho(\mathbf{r},t)\\
&+\frac{1}{4}\varrho(\mathbf{r},t)^4+M(\varrho(\mathbf{r},t))U(\mathbf{r},t)\,\mathrm{d}\mathbf{r}
\end{aligned} \tag{10}$$

with $C = (48\overline{\varrho}^4)^{-1}$, $U(\mathbf{r},t) = (Ck_BT)^{-1}V_1(\mathbf{r},t)$ which is the transformed external potential and with $M(\varrho) := \rho = (1/2)(3-(\varrho/\overline{\varrho}))\overline{\rho}$. This functional is strongly related to the Swift–Hohenberg functional.[9] The evolution equation of the simplified *advected phase-field crystal model* (aPFC) reads:

$$\begin{aligned}
&\partial_t\varrho(\mathbf{r},t)+\nabla\cdot(\varrho(\mathbf{r},t)\mathbf{u}(\mathbf{r})) = \nabla\cdot\left\{\gamma^{-1}M(\varrho)\nabla\frac{\delta\mathcal{F}_1[\varrho(\mathbf{r},t)]}{\delta\varrho(\mathbf{r},t)}\right\}\\
&=: \nabla\cdot\{M(\varrho)\nabla\mu\}\\
&\Gamma^{-1}\mu = (r+(1+\Delta)^2)\varrho(\mathbf{r},t)+\varrho(\mathbf{r},t)^3+M'(\varrho)U(\mathbf{r},t)
\end{aligned} \tag{11}$$

with the diffusion constant $\Gamma := k_B\,TC\gamma^{-1}$.

Computational Results

Numerics

The evolution Equation (6 and 11) are discretized using finite elements in space and a semi-implicit time discretization. For the standard PFC part we follow the approach described in ref.[10] and extend the scheme by a transport term and an external potential. The advection–diffusion equation is discretized using a backward Euler scheme. We use the adaptive finite element toolbox AMDiS[11] to implement the equations.

Similar to the calculation of[2] an external potential of exponential form $(k_BT)^{-1}V_1(\mathbf{r}) = \alpha_1\cdot\exp(-\frac{\|\mathbf{r}\|^l}{\alpha_2})$ is used, where the parameters α_1, α_2, and l are chosen in such a way that the slope and interaction region depend on the colloid and solvent-particle radius. This potential describes a soft colloidal particle in the center of a domain. In our simulations we have set:

$$l := \frac{\ln\left(\frac{\ln(2)-\ln(\alpha_1)}{\ln(\alpha_1-2)-\ln(\alpha_1)}\right)}{\ln(D/R)}, \quad \alpha_2 := D(-(\ln(2)-\ln(\alpha_1)))^{-1/l}$$

for given $\alpha_1 := 10$ and R, D the radius of the colloid and the interaction radius. For simplicity we set the diffusion constant in the evolution equation to $\Gamma = 1$.

Validation

To validate the approach we use a simple configuration with one colloidal particle fixed in the center of a rectangular domain. The flow field is given by

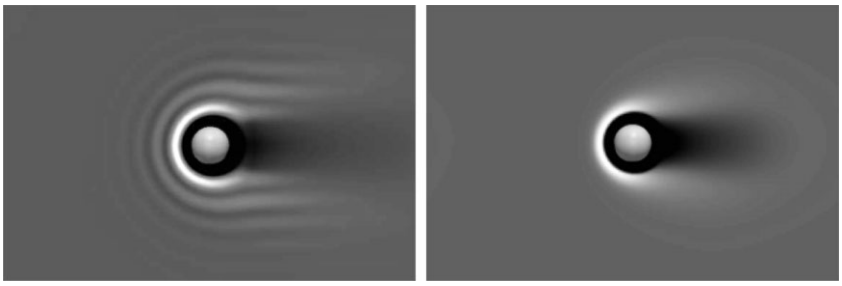

Figure 1. Polymer density around a colloidal particle. Left: Phase-field crystal simulation with $R^* = 0.6$, $c = 0.8$ for the parameters $r = -0.1$, $\overline{\varrho} = -0.3$, right: advection–diffusion simulation with $R^* = 0.6$, $c = 1.0$ for parameter $\overline{\varrho} = -0.3$. Light colors indicate high density whereas dark colors indicate low density. The colloid in the center is visualized as a gray ball.

Equation (1). Figure 1 shows a solution of the advection–diffusion and the advected PFC-equation for a fluid flowing through the domain from left to right. The characteristic first density wave can be seen in both simulations. The studies of refs.[3,12] indicate more than one such wave in the interacting case as can be seen in their Brownian dynamics simulations and dDFT calculations. For this reason we assume that in the interacting case the wave like structure in front of the obstacle is more realistic than the single peak observed in the simple diffusion case.

Proceeding from the qualitative comparison we now follow[2] and analyze the dependency of density on both the radius of the colloid, and the velocity of the fluid, for the case of interacting and non-interacting particles. We use the same analytic Stokes flow (1) with a far-field velocity depending on the reference value $c^* := c^\infty D\overline{\varrho}/r$, that we refer to as the Peclet number. First the radius of the obstacle is fixed at $R/D =: R^* = 0.6$, thus the colloid is bigger than the polymer coils. The size D represents the interaction radius of the colloid, i.e., how close polymer particles can approach the obstacle boundary. The value can be approximated by $D = R + a/2$, where $a = 4\pi/\sqrt{3}$ is the mean distance between polymer particles (constant for our choice of parametrization of the energy), and can be obtained from the one-mode approximation.[7,8] Figures 2 and 3 show the density profile with non-interacting and interacting particles, respectively.

The other relation of density to radius is plotted in Figures 4 and 5, again for non-interacting and interacting particles. Now the Peclet number is fixed at $c^* = 12$. For radii bigger than the polymer coil radius, i.e., $R^* > 0.5$, the density shows an additional wave behind the obstacle, whereas for smaller radii one cannot see such an effect.

Discussion

The difference between Figures 2 and 3 is the formation behavior of the first wave depending on the Peclet number. Where the non-interacting simulation shows a big increase of the first maximum for higher values c^*, in the interacting case this is far less pronounced.

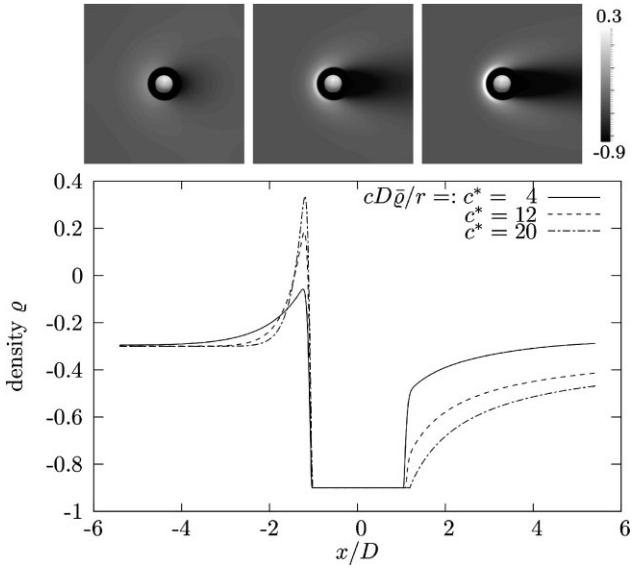

Figure 2. Density-profile of solution with non-interacting particles for different Peclet numbers c^* of the fluid, at fixed radius $R^* = 0.6$ of the obstacle.

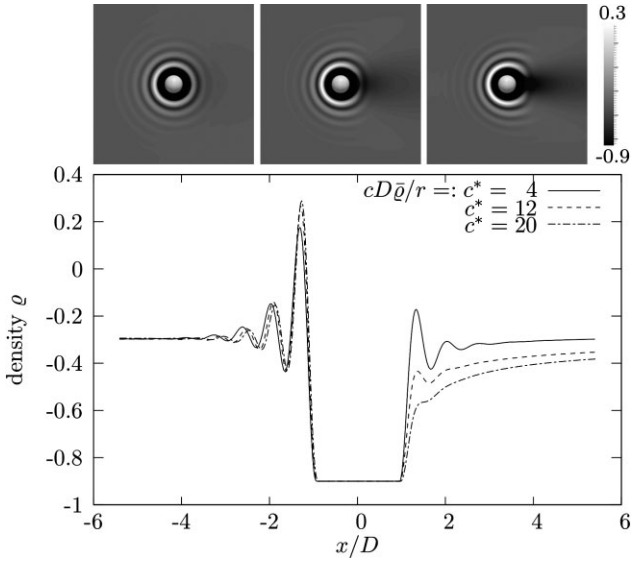

Figure 3. Density-profile of solution with interacting particles for different Peclet numbers c^* of the fluid, at fixed radius $R^* = 0.6$ of the obstacle.

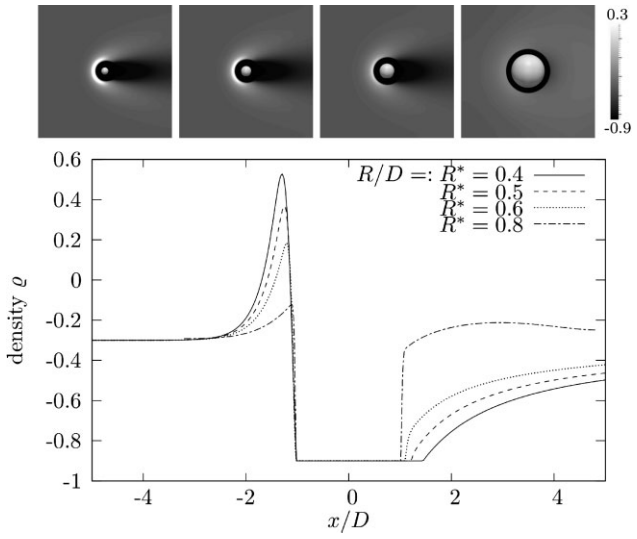

Figure 4. Density-profile of solution with non-interacting particles for different radii R^* of the obstacle, at fixed Peclet number $c^* := 12$ of the fluid.

For the interacting case, the maximum increases slightly with increased c^*, and the change is negligible on further increase of c^*. Behind the colloid, i.e., to the right of the obstacle, the wave structure is also found. Because of the compressibility of the polymer particles in the solvent, the distance of the maxima in front of the colloid shrinks slightly.

The comparison of Figures 4 and 5 goes in the same direction. For higher velocities, i.e., lower values of R^*, the first maximum rises much more in the case of non-interacting particles than in the case of interacting ones. The interesting observation is the structure behind the colloid. For radii R^* less than 0.5, i.e., the colloidal radius is less than the interaction radius of the polymers, the bow wave does not show the oscillating structure, which can be seen for larger radii. The wave is similar to the non-interacting case.

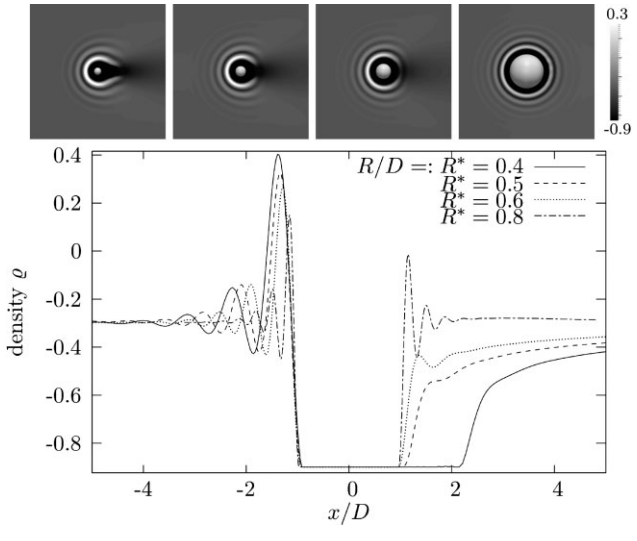

Figure 5. Density-profile of solution with interacting particles for different radii R^* of the obstacle, at fixed Peclet number $c^* := 12$ of the fluid.

Coupling with Navier–Stokes Equation

For more complex configurations of colloidal particles, an analytic result for the flow field can no longer be used. We therefore extend the model and couple the evolution Equation (6 and 11) with a Navier–Stokes equation:

$$\begin{aligned} \partial_t \mathbf{u} + (\mathbf{u}\cdot\nabla)\mathbf{u} &= -\nabla p + \eta\Delta\mathbf{u} \\ \nabla\cdot\mathbf{u} &= 0 \end{aligned} \tag{12}$$

with p the scaled pressure variable and η the kinematic viscosity of the fluid. The problem has to be solved in a domain excluding the colloidal particles. The colloids as macroscopic objects in the flow field have an interaction radius with the fluid approximately equal to R. For fixed colloids the boundary conditions at the colloidal interface are set to $\mathbf{u}=0$. Moving colloids, i.e., moving domain boundaries, need special caution in numerical calculations. We follow the diffuse domain approach in ref.[13] and describe only the geometry implicitly using a phase-field function φ_ε, which indicates the fluid domain by value 1 and the colloidal particles by value 0. Moving colloids can simply be described by shifting the phase-field. A function for the phase-field for one colloid with radius R in the center of a domain can be expressed by a tanh formulation:

$$\varphi_\varepsilon(\mathbf{x}) = \frac{1}{2}(1-\tanh(3/\varepsilon(R-\|\mathbf{x}\|)))$$

where ε defines the width of the diffuse interface and $(R-\|\mathbf{x}\|)$ acts as a signed distance function that defines the boundary as its zero level set and can be replaced by each distance function with negative sign inside the domain. For a set of colloidal particles with position coordinates $\mathbf{r}_i$ the phase-field can easily be adopted by replacing $(R-\|\mathbf{x}\|)$ by a distance function $d(\mathbf{x})$:

$$d(\mathbf{x}) := \max_i\{R-\|\mathbf{x}-\mathbf{r}_i\|\}$$

The diffuse domain Navier–Stokes equations read:

$$\begin{aligned} &\partial_t(\varphi_\varepsilon u_j) + \varphi_\varepsilon\mathbf{u}\cdot\nabla u_j = \varphi_\varepsilon\nabla p - \eta\nabla\cdot(\varphi_\varepsilon\nabla u_j) - \frac{\beta}{\varepsilon^3}(1-\varphi_\varepsilon)(u_j-\bar{g}_j) \\ &j=1,\dots,d \qquad \nabla\cdot(\varphi_\varepsilon\mathbf{u}) = \nabla\varphi_\varepsilon\cdot\bar{\mathbf{g}} \quad \text{in } \Omega \end{aligned} \tag{13}$$

subject to initial and boundary conditions. Thereby β is an additional scaling factor for the penalty term incorporat-

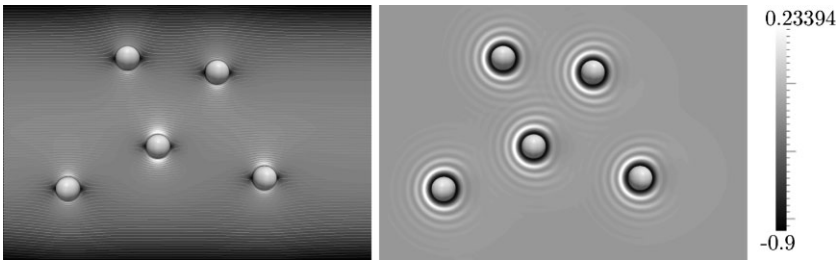

Figure 6. Five colloidal particles as macroscopic obstacles in polymer solution. Left: Streamlines of fluid-particles flowing around the obstacles, red indicates high velocity, blue low velocity. Right: Density profile of particles flowing around the colloids, light colors indicate high densities, dark colors low densities.

ing the Dirichlet boundary condition $\mathbf{u} = \overline{\mathbf{g}}|_{\text{colloid boundary}}$. The approach has already been used and verified for flow problems in ref.[14] and can also be used for situations in which moving colloidal particles are considered. Figure 6 shows an example configuration with five fixed obstacles in a channel with parabolic inflow profile. Analytic results for the flow field could not be found and a numerical approach for the calculation was necessary. The figure illustrates the value of the coupling.

Conclusion

We have proposed a local approximation to the dDFT formulation in ref.[2] The formulation provides an efficient way to treat interacting Brownian particles in a flowing solvent. Neglecting the hydrodynamic interactions between the solute particles and between the solute and colloid particles allows for an efficient coupling, in which only the time derivative in the PFC model is replaced by the total (material) time derivative. The obtained equation thus provides an advected PFC model, which then is coupled to a Navier–Stokes equation in a domain excluding the spherical obstacles.

A quantitative comparison with the full adDFT simulations in refs.[2,3] was not possible. Qualitatively the aPFC simulations show wave structures similar to the results of the authors above, but significantly more pronounced.

The influence of the both Peclet number of the fluid, and radius of the colloidal particle was investigated, and comparison was made between the PFC and diffusion–advection models, for interacting and non-interacting polymer particles in the solvent.

The aPFC model requires much less computational effort than full adDFT simulations, due to the locality of the approach. Furthermore, coupling to the Navier–Stokes equations can be done easily. This is encouraging for extension of the approach to include colloid–colloid interactions in more complex configurations. The calculation of depletion forces between two colloids that are close to each other, so that polymer particles do not fit between them, is appealing and easily realizable with the aPFC approach. Hydrodynamic interactions between the polymer particles is often neglected but could possibly also be included in the model, considering that a weak coupling of aPFC and Navier–Stokes is done already. We are presently working on the inclusion of such interactions.

We have demonstrated that the advected PFC model is a suitable and computationally efficient method for the study of the qualitative behavior of a multicomponent system of polymer and colloidal particles, which influence each other by direct or hydrodynamic interactions, in a solvent.

Received: January 14, 2011; Revised: May 19, 2011; Published online: July 26, 2011; DOI: 10.1002/mats.201100004

Keywords: colloids; dynamic density functional theory; phase-field-crystal; polymer solution

[1] U. M. B. Marconi, P. Tarazona, *J. Chem. Phys.* **1999**, *110*, 8032.
[2] M. Rauscher, A. Domínguez, M. Krüger, F. Penna, *J. Chem. Phys.* **2007**, *127*, 244906.
[3] F. Penna, J. Dzubiella, P. Tarazona, *Phys. Rev. E* **2003**, *68*, 061407.
[4] H. Graf, H. Löwen, *J. Phys.: Condens. Matter* **1999**, *11*, 1435.
[5] T. V. Ramakrishnan, M. Yussouff, *Phys. Rev. B* **1979**, *19*, 2775.
[6] K. R. Elder, N. Provatas, J. Berry, P. Stefanovic, M. Grant, *Phys. Rev. B* **2007**, *75*, 064107.
[7] S. van Teeffelen, R. Backofen, A. Voigt, H. Löwen, *Phys. Rev. E (Stat. Nonlinear, Soft Matter Phys.)* **2009**, *79*, 051404.
[8] K. R. Elder, M. Grant, *Phys. Rev. E* **2004**, *70*, 051605.
[9] J. Swift, P. C. Hohenberg, *Phys. Rev. A* **1977**, *15*, 319.
[10] R. Backofen, A. Rätz, A. Voigt, *Philos. Mag. Lett.* **2007**, *87*, 813.
[11] S. Vey, A. Voigt, *Comput. Vis. Sci.* **2007**, *10*, 57. DOI: 10.1007/s00791-006-0048-3.
[12] C. Gutsche, F. Kremer, M. Krüger, M. Rauscher, R. Weeber, J. Harting, *J. Chem. Phys.* **2008**, *129*, 084902.
[13] X. Li, J. Lowengrub, A. Rätz, A. Voigt, *Commun. Math. Sci.* **2009**, *7*, 81.
[14] S. A. J. Lowengrub, A. Voigt, *CMES: Comput. Model. Eng. Sci.* **2010**, *57*, 77.